

Damage and modification of materials produced by pulsed ion and plasma streams in Dense Plasma Focus device*

Valeriy N. Pimenov,
Elena V. Demina,
Sergey A. Maslyaev,
Lev I. Ivanov,
Vladimir A. Gribkov,
Alexander V. Dubrovsky,
Ülo Ugaste,
Tõnu Laas,
Marek Scholz,
Ryszard Miklaszewski,
Blagoslav Kolman,
Agostino Tartari

Abstract. The Dense Plasma Focus (DPF) devices PF-1000, PF-6 and PF-5M working with different gases and in dissimilar irradiation modes were used to carry out experimental investigations of irradiation of a number of materials by powerful pulsed ion and high-temperature plasma streams. The materials under test were designed for application in structural and functional components of thermonuclear fusion devices with magnetic (MPC) and inertial (IPC) plasma confinement, as well as for working chambers of plasma and accelerator devices. The main features of the materials are low-activation and radiation-resistant properties. On the basis of the investigations a significant progress was achieved in understanding of dynamics of high-energy nano- and micro-second pulsed streams in DPF from one side as well as on the mechanisms of their influence upon materials under irradiation from the other one. We demonstrated that this approach can be useful for certain tests of plasma-facing materials (e.g. W for MPC and stainless steels for IPC) and of structural (construction) elements of the above-mentioned devices subjected to pulsed high-energy radiation streams. The results obtained suggest also that DPF devices can be used in new pulse technologies for material treatment by means of powerful nanosecond and microsecond pulses of plasma and ion streams.

Key words: plasma focus • pulse irradiation • surface damage

V. N. Pimenov[✉], E. V. Demina, S. A. Maslyaev,
L. I. Ivanov
A. A. Baikov Institute of Metallurgy and Material
Science, Russian Academy of Sciences,
49 Leninsky Pr., 119991 Moscow, Russia,
Tel.: +7 095 135 9604, Fax: +7 095 135 8680,
E-mail: pimval@mail.ru

V. A. Gribkov
Moscow Physical Society,
53 Leninsky Pr., Moscow 117924, Russia
and Institute of Plasma Physics and Laser Microfusion,
23 Hery Str., 01-497 Warsaw, P. O. Box 49, Poland

A. V. Dubrovsky
Moscow Physical Society,
53 Leninsky Pr., Moscow 117924, Russia

Ü. Ugaste, T. Laas
Tallinn University,
25 Narva Road, 10120 Tallinn, Estonia

M. Scholz, R. Miklaszewski
Institute of Plasma Physics and Laser Microfusion,
23 Hery Str., 01-497 Warsaw, P. O. Box 49, Poland

B. Kolman
Institute of Plasma Physics ASCR,
3 Za Slovankou Str., P. O. Box 17, 18221 Prague 8,
Czech Republic

A. Tartari
Ferrara University,
12 Via del Paradiso Str, Ferrara 44100, Italy

Received: 14 January 2008
Accepted: 18 June 2008

Introduction

In radiation material science the experimental tests of various specimens of different materials occupy an important niche. In particular it refers to materials which are counted as perspective ones for different parts of plasma devices and accelerators as well as for the mainstream nuclear fusion devices (NFD) of both types – with inertial (IPC) and magnetic (MPC) plasma confinement [3, 9, 14, 15]. In the last category we have to denote first of all those facilities, which are currently under construction – LMJ (France), ITER (France), and NIF (USA). Another issue of the days in this field is to find a proper tool for modification of

* Presented on 3rd Research Coordination Meeting on Dense Magnetized Plasmas, 9–13 April 2007, Beijing, China.

the surfaces of materials with the aim of improvement of their radiation resistance, corrosion resistance and mechanical hardness. In this paper we present a review of the results received for the period of the fulfilment of the 4-year programme of the IAEA Co-ordinated Research Project Dense Magnetized Plasmas together with some new data that have been obtained during the last year and not published yet.

Dense Plasma Focus (DPF) devices are rated as a facility, which can fill a unique niche between devices fitted for these types of experiments [1, 2, 5, 7]. In our previous work [8] three typical regimes of the influence of ion and plasma beams upon a target material placed in the cathode part of DPF device were found in particular: (i) “implantation mode” of irradiation when power flux density of the streams is $q \approx 10^5\text{--}10^7$ W/cm²; (ii) screening of the surface by a secondary plasma cloud – $q \approx 10^7\text{--}10^8$ W/cm² (“detachment mode”); (iii) strong damage with the absence of implantation – $q \approx 10^8\text{--}10^{10}$ W/cm² (“explosive destruction mode”).

In this framework one of the problems is to compare the character of damage and erosion of the surface layers (SL) of various materials (tungsten and several types of austenitic and ferritic steels having different compositions) subjected to pulsed ion and plasma streams of hydrogen isotopes in dissimilar irradiation conditions. In particular, stainless steels were elaborated with the purpose of a reduced ability to be activated by neutrons. The importance of the work is also connected with the fact that tungsten is plasma-facing material in ITER, whereas ferritic-martensitic steels are used as plasma-facing materials in devices with IPC and intended for structural components of ITER. Moreover, these steels may be more perspective for the use in next generation of NFD compared to the accepted ones for contemporary generation. Austenitic steels, duralumin, and vanadium are utilized in working chambers of different plasma devices and accelerators as well. Pure iron and aluminum were selected to compare defects produced on them with those created on steels and duralumin surfaces.

Our experiments were performed with the use of devices PF-1000, PF-6 (both of Institute of Plasma Physics and Laser Microfusion, Warsaw, Poland) and PF-5M (A. A. Baikov Institute of Metallurgy and Material Science RAS, Moscow, Russia). The working gases in the PF-1000 facility were two hydrogen isotopes: hydrogen and deuterium, whereas in the PF-6 apparatus it was deuterium. We use only hydrogen in the PF-5M device.

Scanning electron and atomic force microscopy as well as X-ray diffraction analysis were carried out in col-

laboration with the Institute of Plasma Physics (Prague, Czech Republic), Tallinn University (Tallinn, Estonia) and Ferrara University (Ferrara, Italy).

The results of study of the influence of pulsed powerful streams taking place in the PF-1000, PF-6 and PF-5M devices upon damage, mass transfer, evolution of microstructure, and subsequent properties of the above materials are given below. On the basis of these results the prospects applying of Dense Plasma Focus devices for solving scientific and applied problems of radiation material science are discussed.

Materials and radiation conditions

Samples of austenitic and ferritic steels were smelted in the form of ingots, rolled up to 0.1 cm thick and made in the form of plates having a size of $1.5 \times 1.5 \times 0.1$ cm³. The chemical compositions of the steels are given in Table 1. The power flux density q of plasma and fast ion streams irradiating the target materials was in the range of $10^7\text{--}10^9$ W/cm². Ferritic steel Eurofer-97 and pure Fe was irradiated under harder conditions, namely at $q \sim 10^9\text{--}10^{10}$ W/cm². Sintered tungsten specimens prepared by means of powder metallurgy as sticks of square section 11×11 mm² were also tested under irradiation. The purity of W was 99.95% with some additives and impurities (Fe, Ca, C, N, H, O). The tungsten stick was cut as plane-parallel plates of 2 mm thickness. Irradiation power density in these experiments was $q = 10^8\text{--}10^{10}$ W/cm². Pulse durations τ were about 0.5...3 μ s in PF-1000, and 30–100 ns in PF-6 and PF-5M devices. We used PF-1000 with 1 pulse per 15 min and PF-6/PF-5M 1 pulse per 3 min, correspondingly.

Results of plasma-beam observations

The Dense Plasma Focus device known since the mid-1950s is one of the most accurately diagnosed facilities. Many of its parameters were measured with ns temporal and 10- μ m spatial resolutions. Yet some of its features still demand a better characterization and interpretation. Among them are a more precise description of plasma streams dynamics having a speed about $(1\text{--}5) \times 10^7$ cm/s and a beam of fast ions (with energy equal to about 100 keV) is necessary. Our experiments made with a frame camera, which takes an image of plasma self-luminosity in the visible range with a time exposure of 1 ns, have shown new data some of which were presented in Ref. [6]. Among them in our devices we could trace a sequence of events taking place both

Table 1. Chemical composition of the steels

Steel	Content, mass%									
	C	Cr	Mn	Si	W	V	Ta	N	P	S
10Cr12Mn20W	0.10	12.10	20.10	0.02	2.05	–	–	0.010	0.02	0.02
25Cr12Mn20W	0.25	11.57	20.75	0.02	2.01	0.10	–	0.003	0.04	0.008
10Cr12Mn20W + (0.05%La)	0.10	11.90	20.10	0.02	2.05	–	–	0.002	0.02	0.02
10Cr12Mn20W + (0.05%Sc)	0.10	11.90	20.10	0.02	2.05	–	–	0.002	0.02	0.02
30Cr10Mn33W	0.30	10.00	33.00	–	1.00	1.00	–	–	–	–
10Cr9WV	0.11	9.20	0.65	0.30	1.00	0.15	0.10	0.030	0.02	0.007
Eurofer-97 Ni-0.021	0.11	9.00	0.48	–	1.10	0.20	0.07	0.030	0.005	–

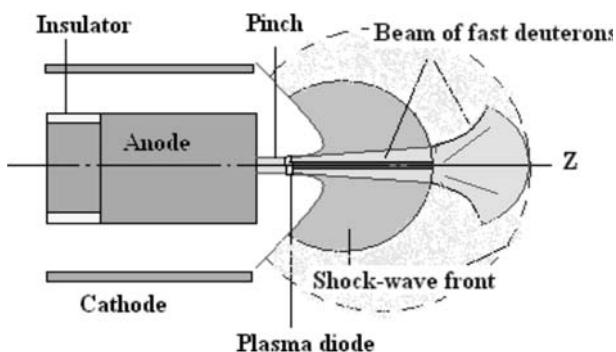


Fig. 1. Scheme of dynamics of plasma streams and fast deuteron beams in the PF-1000.

in primary (pinch) and secondary (target under irradiation) plasmas, which looks as follows (see Fig. 1):

- After plasma pinching near the Z-axis of the DPF chamber on the top of the anode of the device, a shock wave (SW) is formed by an axial cumulative plasma jet in the residual gas above the pinch.
- This SW propagates as a hemispherical structure above the pinch in the direction of Z-axis from the anode.
- Some period of time later a plasma diode is formed in the pinch plasma, which produces at first a powerful beam of fast electrons directed along Z-axis to the anode and later a powerful beam of fast ions (energy of particles ~ 100 keV) propagated into the opposite direction.
- The central (most energetic) part of the fast ion beam (“core”) propagates in a very narrow angle (a few degree $\sim 3^\circ$) within the space between the pinch and the SW front whereas its part which holds the lower amount of energy has a divergence about 30° (like in Fig. 1).
- This ion beam is scattered noticeably into a full solid angle after its penetration through the SW front because of inductance inherent to it and due to the absence of its charge and back-current compensation in this low-density neutral gas region.

Spectroscopy of the secondary plasma made for tungsten/carbon-fibre-compound in the visible range with 1- μ s time resolution at the PF-1000 facility has shown that ([6]):

- In the visual range there are lines of deuterium and multi-stripped ions of carbon, but there are no lines of W; this means that the temperature of the secondary plasma is very high.
- Low ionized copper (produced on the anode by electron beam) appears near the target placed at a distance of 30 cm from the anode only 30 μ s later in comparison with the deuterium plasma luminescence; this means that the velocity of copper plasma stream is about 10^6 cm/s and its corresponding temperature near the anode was about 100 eV.
- The time of existence of the secondary plasma near the surface of the sample is about 100 μ s.

Physics of the ion beam scattering after its penetration through the shock front is quite clear. Indeed, to preserve good transport of a high-current ion beam through medium we have to fulfil charge and current neutralization of it along its way. Ion density in our beam is about 10^{16} cm $^{-3}$ [4]. Background plasma is

formed by a combination of a cumulative plasma stream (jet) produced in the DPF during first compression and of plasma compressed and ionized in a shock wave (SW) behind its front. Thus, its density is about an order of magnitude higher than the ion beam density value. On the contrary, the density of the plasma produced ahead of the SW front by the ion beam itself has the same value as in the beam or lower. That is why both types of neutralization are possible only on the backside of the shock wave and they are violated ahead its front.

Radiation and thermal effects

The experiments performed with different types of PF facilities [10, 11, 13, 16–20] show that the influence of pulsed high-energy ion beam ($E_i > 100$ keV) and dense plasma (velocity of the particles is about 5×10^7 cm/s) on the target materials lead to a remarkable difference in radiation and thermal effects depending on irradiation conditions in the PF chamber. Parameters of radiation affect the character of the physical and chemical processes in the materials tested, the damage of their surface layers (SL) and phase-structural changes in it.

DPF, producing relatively short pulses of ion beam and plasma stream (as it was mentioned above), ideally may simulate conditions in the main-stream of thermonuclear devices with IPC [14] (except the total energy used, as in those facilities radiation is spread into full solid angle whereas in DPF we produce narrow directed streams). However, it may also be very useful in facilities with MPC like a tokamak in some aspects of the radiation damage tests. There are two factors which have to be taken into account in this connection:

1. Primary plasma and a beam of fast ions irradiate a target in DPF during a short interval of time (from 100 ns till few microseconds) compared with transient events taking place in a tokamak (e.g. ELMs). But secondary plasma produced by them at the target surface loses its density (two orders of magnitude) and temperature (down to a few eV) during 100 μ s. And one has to take into account that the temperature of a few eV means a few tens of thousands of degrees, what is much higher than a metal melting point. This means that thermal load in our case has a duration which is close to that produced in a tokamak during transient events. And what is especially important – in DPF we have radiation of the same type – plasma and fast ion streams – and having the same parameters as in the contemporary tokamaks near the chamber wall: plasma temperature = 1 keV, energy of fast ions = 100...200 keV, i.e. the same as used for neutral beam plasma heating. This is in contrast to the situations, which are realized at present in a number of laboratories, where the simulation tools sometimes having nothing in common with the real radiation types and their parameters in tokamak.
2. Discussed in a number of papers the so-called damage factor: $F \sim q \cdot t^{1/2}$ (where q is the power flux density and t – pulse duration of radiation) gave us another opportunity (see e.g. [16, 17, 19, 20]). Because our DPF devices can produce power flux density at least 2–4 orders of magnitude higher than

all the contemporary instruments used in radiation material tests (electron and ion beams, plasma accelerators) we may ensure the same magnitude of F having pulse duration of radiation 4–8 orders of magnitude shorter. In these conditions many features of radiation damage, taking place in relatively long events, can be reproduced with our devices even with these short pulses.

Moreover, in connection with this damage factor and having such a powerful source of radiation (DPF) there is an intriguing point to be verified in future experiments: whether it would be possible to execute radiation tests of different candidate materials during a very short experimental session rather than to provide a long-term examination of them during time intervals equal to a real tokamak exploitation campaign?

Radiation effects under the conditions considered here are mainly connected with the sputtering of the irradiated material and the formation of surface and bulk structural defects. Thermal effects induced by the high energy pulsed action on the material become apparent chiefly in the processes of melting and recrystallization, evaporation, boiling and also heat- and mass-transfer. Under radiation conditions realized in DPF devices the thermal effects, as a rule, dominate over radiation phenomena. All together radiation and thermal pulsed

influences resulted in the damage and erosion of the surface layer of the target material as well as in changing its phase-structural state and properties. Let us examine results of investigation of these phenomena produced in our experiments in confrontation with elemental content of working gas, irradiation of specimens by fast plasma streams only or together with the beams of fast ions, with variations in power flux density as well as with material of specimens and its disposition in relation to the irradiating streams.

Features of surface layer damages

Analysis showed that the character of the surface damage and the relief of the irradiated surface depend on both irradiation mode (working gas composition, power flux density and pulse duration) and thermal properties of the target material.

Investigations of austenitic and ferritic steels (see Table 1) after irradiation showed that the irradiation resulted in melting, evaporation, sputtering and sometimes crack formation on the surface layer. The remelted surface always had a wave-like relief with different defects: craters, influxes, droplets, pores, microcracks, etc. [11, 16, 17]. Figures 2 and 3 present

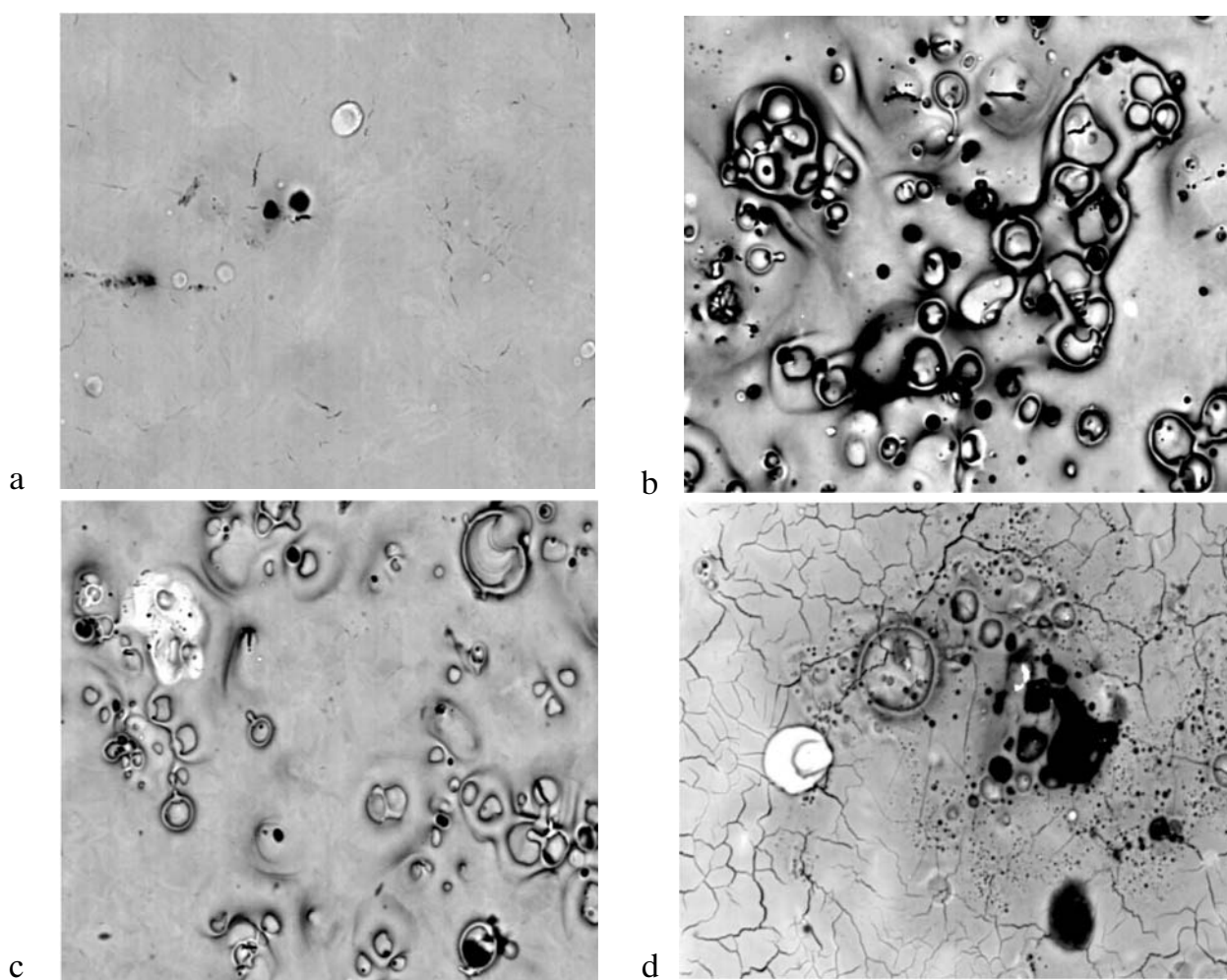


Fig. 2. Scanning electron microscopy of the surfaces of austenitic steels irradiated in the PF-1000 device by deuterium plasma: a – 10Cr12Mn20W (8 pulses); b – 25Cr12Mn20W (8 pulses); c – 10Cr12Mn20W+0.05Sc (5 pulses); d – 10Cr12Mn20W+0.05La (5 pulses); $q \approx 10^8$ – 10^9 W/cm².

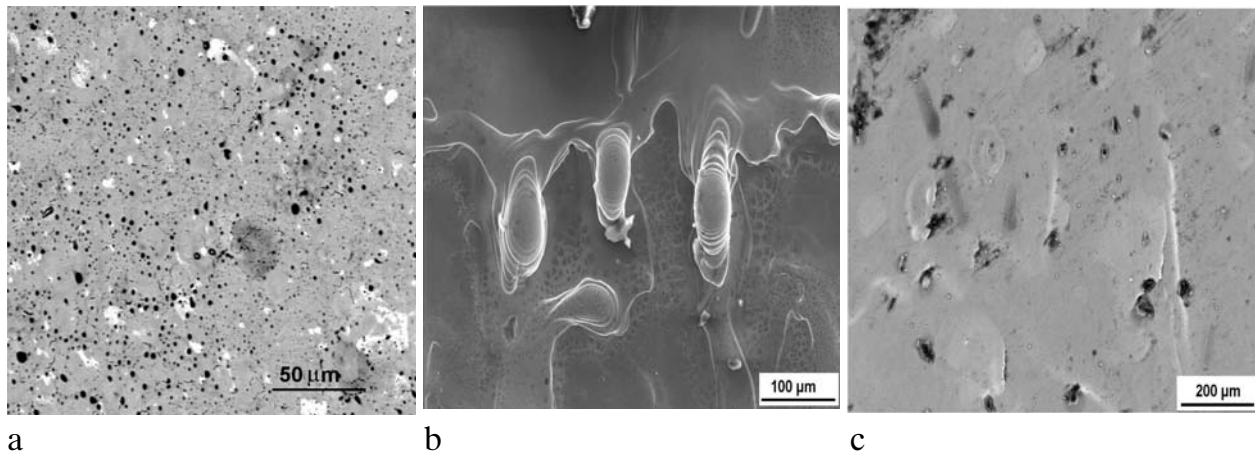


Fig. 3. Scanning electron microscopy of the irradiated surfaces of ferritic steels: a – 10Cr9WV (PF-1000, 8 pulses); b – Eurofer-97 (PF-6, 8 pulses); c – Eurofer-97 (PF-1000, single pulse); $q \approx 10^8\text{--}10^{10}$ W/cm².

Table 2. Changes of mass of steel specimens under irradiation

Material	Number of pulses	Total mass loss Δm (mg)	Mass loss per pulse (mg)	Mass loss per square unit (mg/cm ²)	Thickness of evaporated layer per one pulse (μm)
Steel 25Cr12Mn20W	8	0.30	0.0375	0.531	0.67
Steel 12Mn20W	8	0.25	0.03125	0.442	0.56
Steel 10Cr12Mn20W doped with La	5	0.29	0.058	0.821	1.04
Steel 10Cr12Mn20W doped with Sc	5	0.10	0.0200	0.283	0.36
10Cr9WV	8	0.35	0.04375	0.619	0.78
Eurofer-97	1	0.75	0.75	1.785	2.26
Eurofer-97	8	+0.35	+0.044	+0.044	–

the scanning electron photos of irradiated surfaces of the steels listed in Table 1. These figures show that surfaces of all ferritic steels (Fig. 3) and of one sort of austenitic steel 10Cr12Mn20W (Fig. 2a) are less damaged compared to other austenitic steels. They contain the least number of defects (mainly pores, droplets and spots of copper redeposited from the DPF anode). The surfaces of other specimens (in addition to the noted defects) have numerous craters, bubbles, open bubbles and microcracks (Figs. 2b, 2c, 2d). Analysis showed that irradiation resulted also in erosion of the materials, mass loss and reduction of the specimen thickness compared to their initial state.

Table 2 presents the results of weighing the steel specimens before and after deuterium plasma irradiations as well as a calculation of the layer thickness d evaporated during a single pulse (last column) based on weighing and specific density of each material. The given values of d are somewhat lower than those received from estimations for the thermal load in these irradiation conditions in DPF because in these estimations the redeposition of the copper from the anode and other elements from the parts of PF chamber to irradiated surface were not taken into account. The fact that the redeposition took place in these experiments resulted from the observation of even the mass increase of Eurofer-97 steel specimen after irradiation in the PF-6 device in one particular test (see Table 2, last line). Usually, it happens when no special measures is produced (like installation of a hollow DPF anode, an operation in the regime with low electron beam production in DPF, etc.).

Nevertheless, from the results received we can conclude that under irradiation with $q = 10^8\text{--}10^9$ W/cm²

austenitic steel 10Cr12Mn20W doped with lanthanum has the lowest resistance to erosion. Under the realized irradiation conditions this steel was liable to enhanced crack formation (see Fig. 2d) that lead to reduction of heat transfer from the surface to the bulk and increase of surface erosion.

For all the test specimens (except steel Eurofer-97, which was irradiated under harder conditions) the thickness d and the mean projective path R_i of fast ions (with energy $E_i \approx 100$ keV) are connected by the relation $d \leq R_i \approx 1 \mu\text{m}$ [21]. This means that deuterium ions were implanted into the target material [8]. Steel Eurofer-97 was irradiated under the conditions of “explosive rupture implantation” and for this regime the irradiation condition was $d > R_i$ (see Table 2). This means that the implanted deuterium ions were removed from the material together with the evaporated layer.

Our experiments have shown that the relief changes on irradiated surfaces depends not only on radiation power flux density and material properties, but also on the orientation of a specimen to the irradiating stream. For example, the outer surface of the tubes placed along the axis of the chamber of the PF device [18, 20] was damaged remarkably less than the surfaces of the specimens positioned normally to the plasma stream at the same distance from the DPF anode (compare Figs. 2 and 4). The surface of the tubes had significantly fewer surface defects, mainly droplets and influxes. A similar situation was also observed on the irradiated surface of a duralumin tube [18, 19]. Indeed, Fig. 5 shows the surface relief, which is covered with surface imperfections like droplets, influxes and ridges (but no craters, blisters,

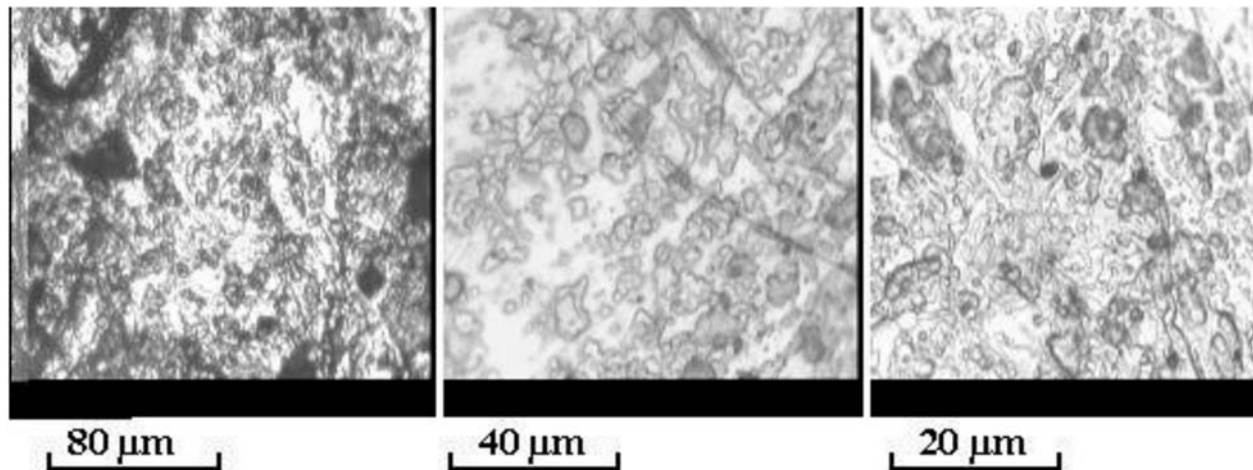


Fig. 4. Parts of the external surfaces of the tube 10Cr12Mn20W at the “hot” zone (PF-1000, 4 pulses, deuterium plasma); $q \approx 10^7$ W/cm².

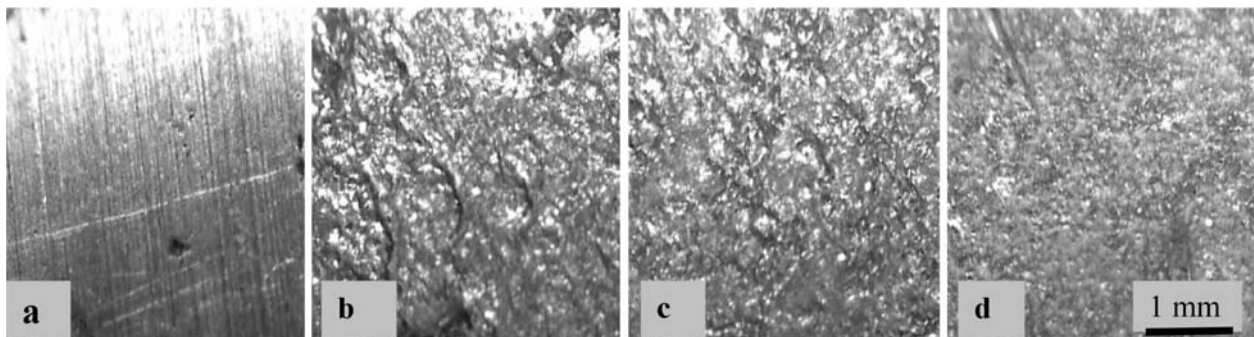


Fig. 5. Topographic structure of the surface of a duralumin tube in the original state (a) and after 13-fold pulses of deuterium plasma: b – part the nearest to the anode; c – central part; d – part the farthest from the anode; $q \approx (1-5) \times 10^6$ W/cm².

and other surface defects). This is a clear consequence of lower power flux density in this geometry.

Large ridges formed in the zone of irradiation with high power density (Fig. 5b) are curved in the direction of the plasma stream. The extension of the ridges and the distance between them are about hundreds of micrometers. Typical size of relief details (ridges, droplets and influxes) decreased with distance from the anode. The velocity of the particles (both in the plasma

stream and especially in the fast ion beam) is very high. This means that the momentum input is also very high, which might be the reason for melt layer movement observed in the experiments.

At the same time, it should be marked that in the case of placing a flat specimen by its surface normally to the incident stream the microcracks appeared not only on the surfaces of the austenitic steels (at $q = 10^8$ W/cm² for plasma streams like in Fig. 2d) but also

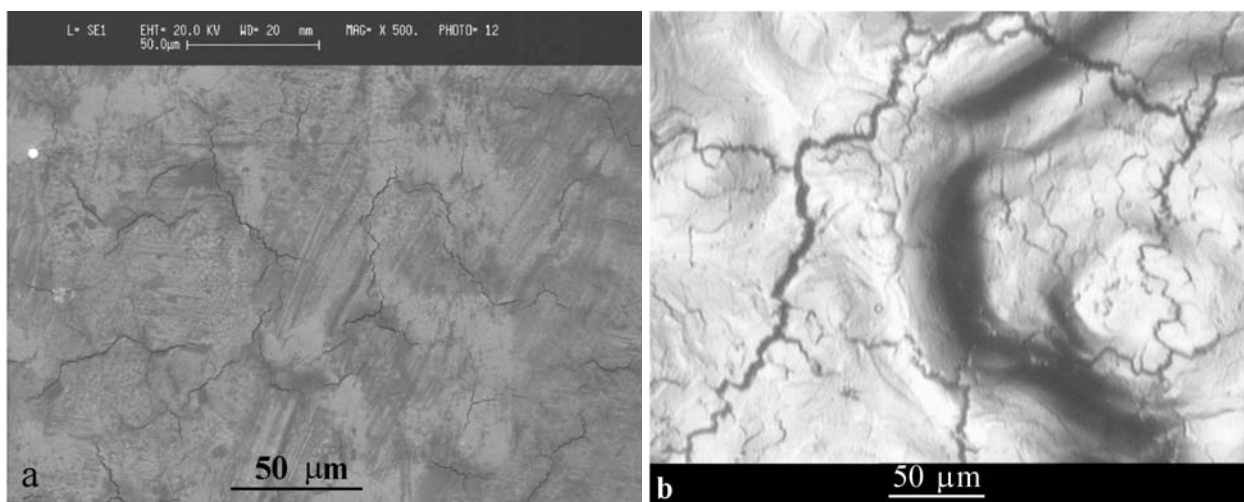


Fig. 6. Microcracks on the surfaces of irradiated vanadium and tungsten: a – electron scanning image of the part of the vanadium sample surface after 3 pulses of hydrogen plasma beams ($q = 10^8$ W/cm²); b – optical microscopy image of the part of the tungsten sample surface after 10 pulses of the deuterium plasma and ion beams (with $q = 10^{10}$ W/cm²).

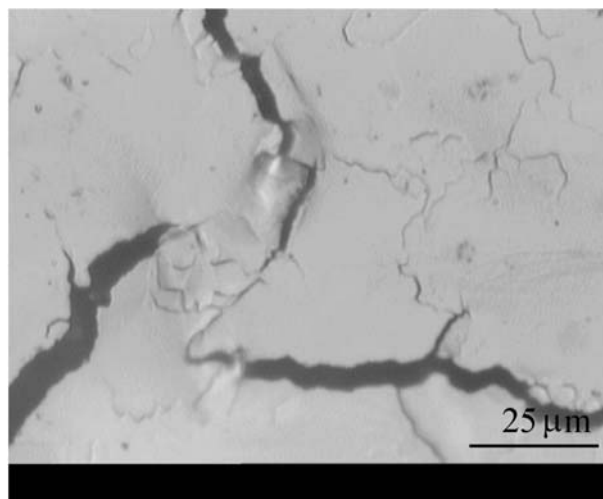
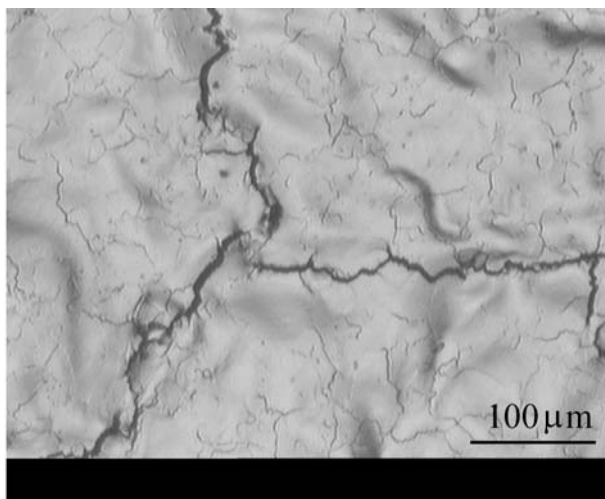


Fig. 7. Microcracks on the irradiated surface of tungsten after 10 pulses of the deuterium plasma ($q = 2 \times 10^8$ W/cm², optical microscopy).

in more refractive materials – vanadium and tungsten (Fig. 6). For both these materials, an intercrystalline fracture at the surface took place. In vanadium samples irradiated only by hydrogen plasma in the PF-1000 facility it happens at a level of power flux density of the order of 10^8 W/cm² [17]. But in tungsten specimens, this microcracks formation was observed in more severe regimes when these samples were irradiated either only by plasma streams as above, but at the power flux density $q = 10^9$ W/cm², or in the case of action of both hot plasma streams and beams of fast ions at $q = 10^{10}$ W/cm² (see Fig. 6b and Fig. 7). This formation of microcracks shows that thermal stresses inside the surface layers of the specimens appeared at the irradiation override of the material breaking point. Taking into consideration the particular shapes of the microcracks in the W and V specimens (Figs. 6, 7) as well as in austenitic steel with lanthanum doping (Fig. 2b), one may conclude that this cracking of the surface layer follows the mechanism of “brittle fracture”. Estimation of the erosion of the irradiated W specimen, which has been prepared by a powder technique, showed that the single-pulse irradiation by deuterium ions and plasma at the power flux density $q = 10^{10}$ W/cm² resulted in the evaporation of the layer having its thickness $d \approx 2$ μm.

Taking into account the fact that tungsten is planned for use as an armour material for divertor plates in ITER, the results obtained may be useful for preliminary prediction of the material behavior in extreme situations for plasma disruption in NFD.

As it is seen from the above-mentioned results, one general feature of the dissimilar materials irradiated in different conditions is their pronounced wave-like relief. We are of the opinion that this character of the surface modification may be useful for application of them in the internal plasma-facing components in future NFD. Indeed, we deem that the formation of the rippled surface (close to the needle-shaped one) on the above-mentioned armour plates will promote two important qualities of them:

- Lower accumulation of gaseous substances in the material due to enhanced outward diffusion of them through highly developed (three-dimensional) surface (thus having much larger area).

- Reduced sputtering of it in comparison with the flat surface, because in this case the process will take place only on the peaks of ripples, whereas the material evaporated from the side-on surfaces of the “needle” will be redeposited onto the adjacent side-on areas (in the self-supporting regime as we can see in these experiments).

Surface layer alloying

Specific defects are formed on the irradiated surface of the test specimen owing to the deposition of different materials placed in the PF chamber. If the material is deposited in the form of droplets (for example, after the action of a power electron beam on the copper anode surface [17, 20]), then it covers the surface with a great number of spots (see Fig. 8). Under multifold irradiations the deposited material can mix up with the liquid phase; it can lead to alloying the surface layer more uniformly. If the material is deposited in the form of an ion or atom stream, then it is dissolved in the liquid phase as the element of a dopant and alloys the surface layer relatively uniformly, too. It is clearly seen in Fig. 9, and it is dissimilar to that shown in Fig. 8. Thus, in both cases a copper-rich layer uniformly covers the central part of an irradiated specimen, which did not contain copper in the initial state.

As we have already mentioned above, such sputtering and redeposition of materials from the DPF anode can be “switched on” or “switched off” to a considerable degree by a number of measures at will. And, e.g., for experiments on the radiation test of materials intended for NFD based on MPC, we may eliminate any redeposition (except working gas) or just opposite to use beryllium (plasma-facing material) as an anode insert for its sputtering.

Thus, in addition to the possibility of the implantation of the working gas ions [8] the plasma focus devices allow us to alloy the irradiated surfaces under the action of ion and dense plasma streams of different elemental content. It may improve, e.g., the mechanical properties and corrosion resistance of the material. In this way the results obtained here

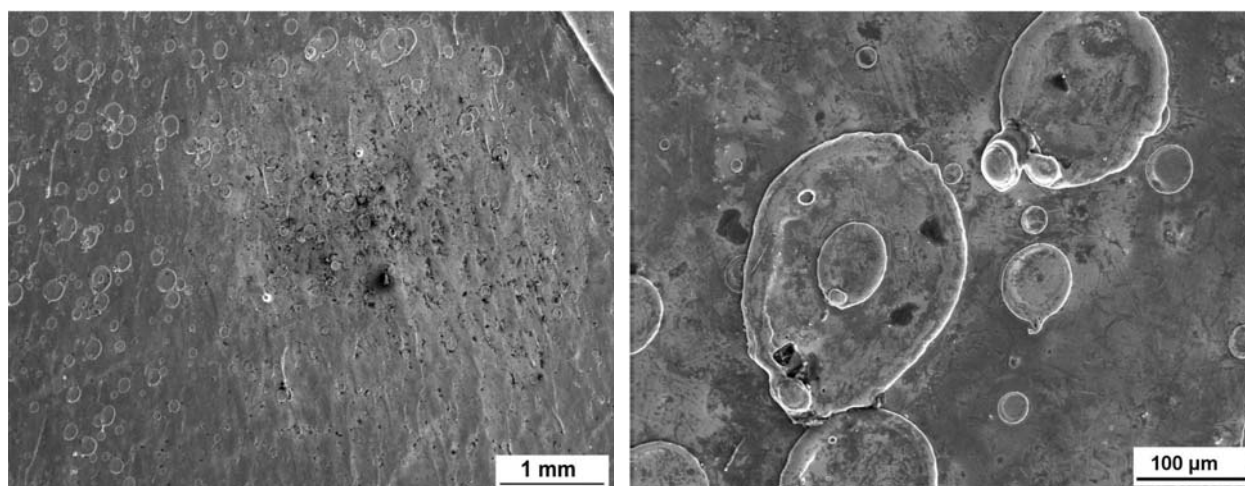


Fig. 8. Irradiated surface of pure iron after deuterium plasma irradiation in the PF-1000 device (single pulse, $q = 10^9$ W/cm²). Copper spots are clearly seen.

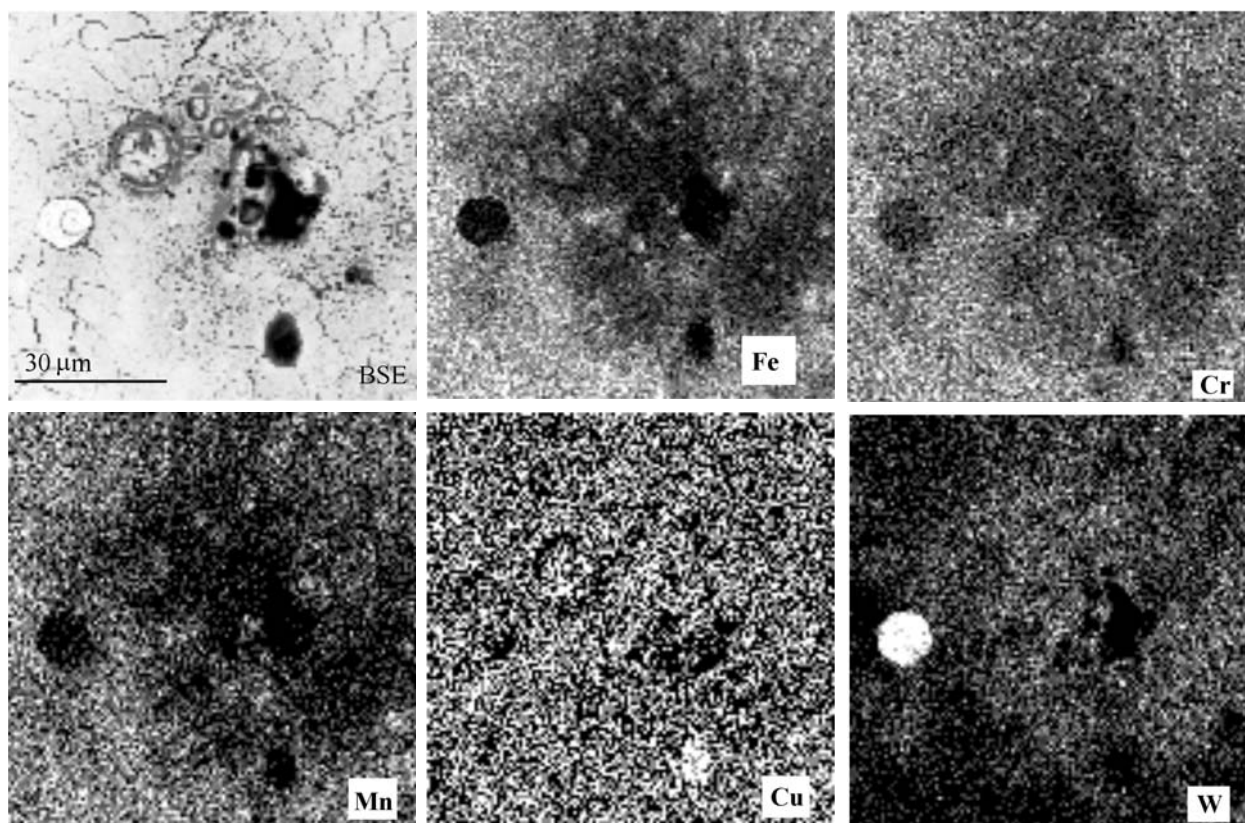


Fig. 9. The surface of steel 10Cr12Mn20W + 0.05%La irradiated with 5-fold pulsed action of fast deuterium ions and plasma streams (back scattering electrons and characteristic X-ray); $q \approx 10^8$ W/cm².

show that the Plasma Focus devices may not only be used for investigation of radiation and thermal effects but also for the estimation and forecast of radiation resistance of materials under investigation as well as for the development of new techniques of pulsed ion treatments of materials.

Structural and phase stability

The investigations of structures of irradiated specimens in cross-section show that the influence of pulsed ion and dense plasma beams result in the change of microstructure and sometimes in the phase-structure state of

the surface layer. As a rule, the reduction of the grain size in the surface layer in comparison with the initial state and formation of microstructures with typical grain sizes in the range from tens of nanometers to a few micrometers were observed. This fact is connected with the high cooling rate of the liquid phase ($\sim 10^6$ – 10^8 K/s) after pulsed action [18, 19]. Examples of disperse microstructures in recrystallized surface layers for the steel tube 25Cr12Mn20W tested and for pure Al and Al-alloy are given in Figs. 10–12 [18, 20]. In Fig. 10, one may see microphotography of the irradiated parts of the tube manufactured of 25Cr12Mn20W at its central region in the zone of initial material (1), as well as external (2) and internal (3) surface layers. Grain size

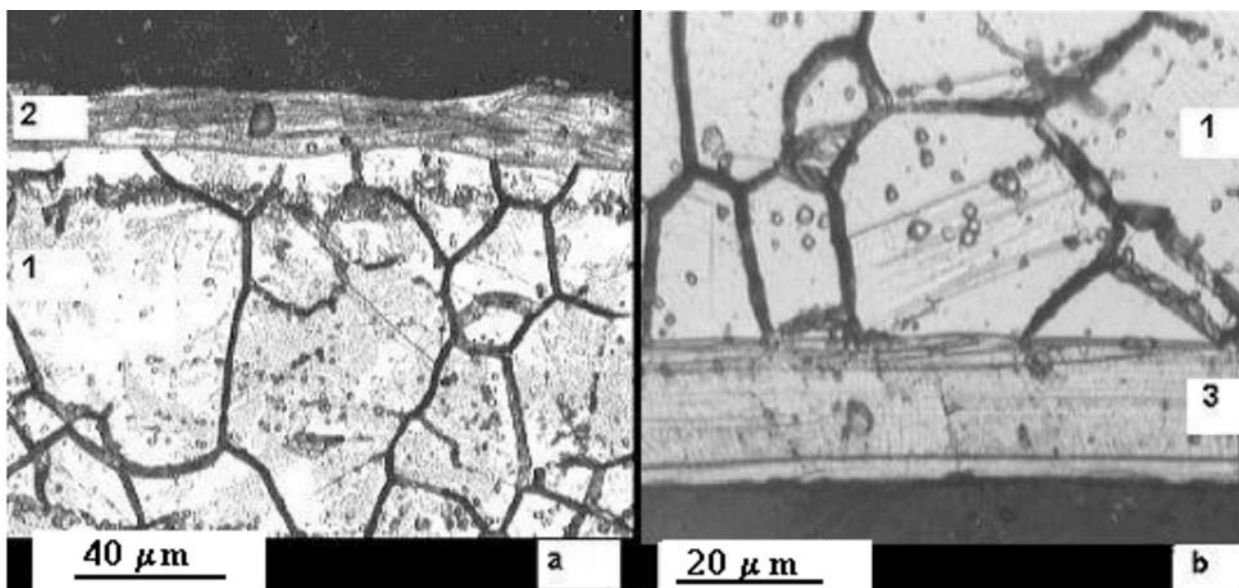


Fig. 10. Cross-sections of the steel tube 25Cr12Mn20W at the central part after 4 pulses of the deuterium plasma ($q \approx 10^7$ W/cm²): a – zone of outer surface layer; b – zone of inner surface layer; 1 – initial microstructure; 2 – recrystallized layer of the outer surface; 3 – recrystallized layer of the inner surface [20].

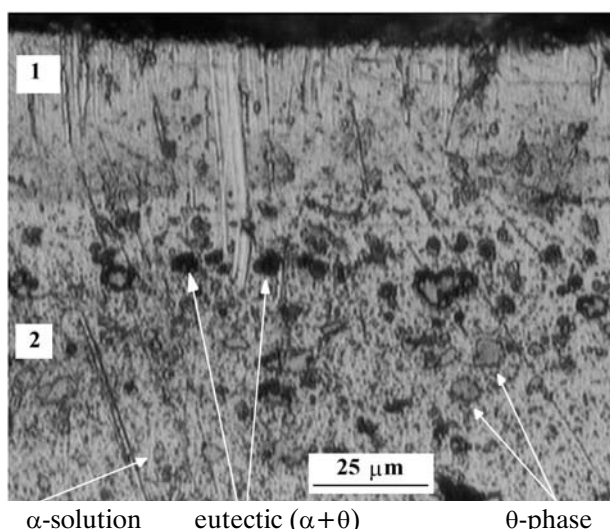


Fig. 11. Cross-section of the surface layer of a duralumin tube after 13 pulses of the deuterium plasma: 1 – recrystallized surface layer; 2 – initial structure ($q \approx 2 \times 10^6$ W/cm²).

refinement, as a rule, results in changing the mechanical properties of the surface layer.

The changes of phase-structural states of the materials after the action of ion and plasma pulsed beams was studied for austenitic steels and Al-based alloy. In steels 10Cr12Mn20W and 25Cr12Mn20W there appeared under irradiation dispersive inclusions of α -phase in austenitic (γ -phase) matrix (see Fig. 13). It is seen that the irradiation results in structure-phase transformation in the surface layers. In irradiated specimens we observe the reduction of (111) γ , (200) γ , (220) γ and (311) γ peaks and the appearance of α -phase peaks, which correspond to the martensite structure.

At the same time, the tested ferritic steels 10Cr9WV and Eurofer-97 (see Table 2) did not show any phase transformation $\gamma \rightarrow \alpha$. The phase composition of these steels after multifold action of powerful deuterium plasma pulses has not been changed. This result is important for estimating the prospects of applying ferritic-martensitic steels in thermonuclear reactors with magnetic and inertial plasma confinement.

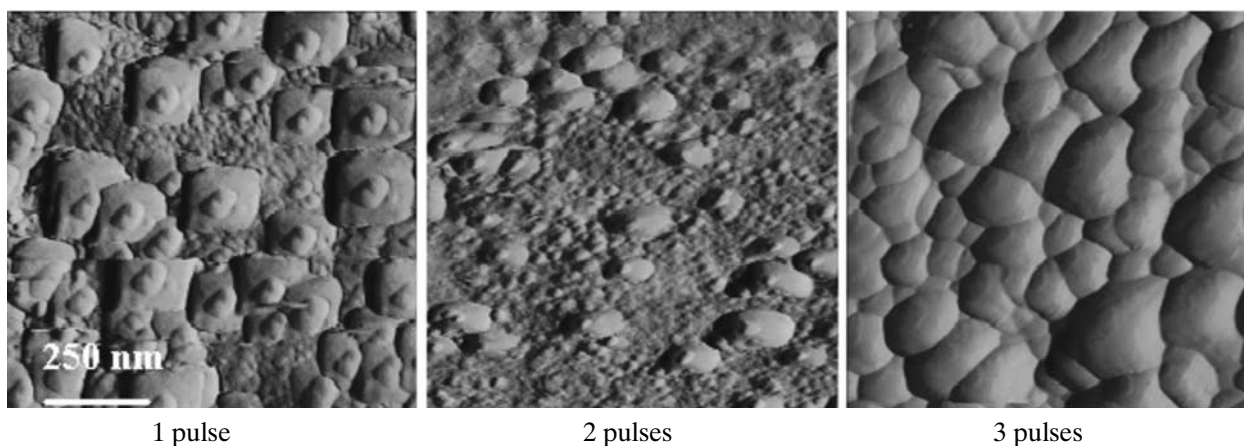


Fig. 12. Surface topography of Al surface after irradiation with deuterium ion and plasma beams in the PF-1000 device ($q \approx 10^7$ W/cm²); atomic force microscopy.

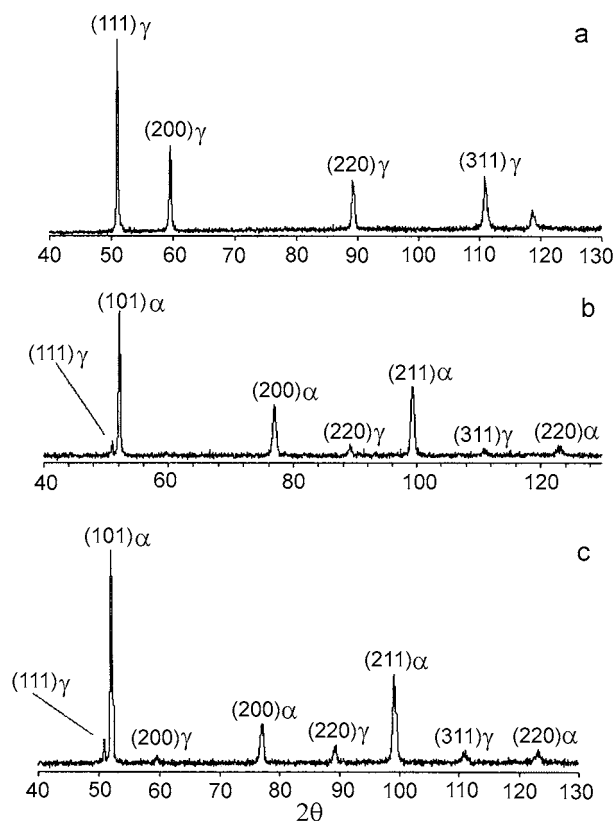


Fig. 13. X-ray diffraction patterns for the irradiated steel 10Cr12Mn20W tube in the initial state (a) and after 4 pulses of deuterium plasma actions: b – outer surface layer; c – inner surface layer; $q \approx 10^7$ W/cm².

The Al-based alloy in the initial state had a double-phase structure [18, 19] and consisted of α_{Al} – solid solution and inclusions of the second phase $CuAl_2$ (θ -phase). After plasma irradiation, there appeared two zones (see Fig. 11): (i) recrystallized α_{Al} layer, where θ -phase inclusions were practically completely dissolved; (ii) adjacent (transition) zone with inclusions of θ -phase and eutectic (α_{Al} + θ -phase). The structural and phase transformations observed as well as the formation of the microcrystalline structure induced hardening and strengthening of the surface layers.

On the whole, we can conclude that the evolution observed in the phase-structural states of the surface layers after their irradiation shows the differently directed consequences of the irradiation of materials under tests for their use in fusion/plasma/accelerator devices and for other applications. From the one side, we may see the possibility of applying the material treatment with power pulses in PF devices to improve mechanical properties and corrosion resistance of materials. The above results suggest also that erosion and accumulation of gases in plasma-facing materials inside the NFD on the wave-like relief of their surface irradiated beforehand can be reduced. It is connected with partial redeposition of material evaporated from droplet-like surface mainly to the side surface of the droplets and with an increase of the gas diffusion through increased area. Besides, the increase of the total grain boundary area with the formation of dispersive structures in the surface layer results in the increase of concentration of the crystal lattice defects (dislocation, lattice distortion,

etc.). That induces generation of sinks for radiation defects and positively reduces blistering under irradiation [12]. But from the other side, this increase of lattice defects may lead to larger tritium retention, which is most unwanted for fusion materials.

Conclusions

The Plasma Focus devices PF-1000, PF-6 and PF-5M with different gases and different irradiation modes were used to carry out experimental investigations of the interactions between pulsed high-temperature plasma streams and beams of fast ions and a number of materials to be applied in plasma facing (armour), structural and functional components of thermonuclear fusion devices with magnetic and inertial plasma confinement, as well as for working chambers of plasma devices and accelerators.

On the basis of the investigations carried out, a significant progress was achieved in understanding the dynamics of plasmas/fast ion streams within DPF and the mechanisms of the influence of high-energy nano- and microsecond pulsed beams upon irradiated materials.

It was shown that the main factors for damage of materials under high-energy pulses in PF devices are heat loads resulted in melting of the irradiated surface layers, erosion of materials (mass loss by evaporation and thinning of samples), formation of different types of surface defects (droplets, influxes, pores, craters, bubbles, open bubbles, etc.) and formation of microcracks. The degree of material damage depends on the power flux density of the radiation streams and on the orientation of the irradiated surface in relation to the beams. Maximal damage is observed when the beam is normal to the surface and the irradiated specimen is in closest position to the pinch thus ensuring power flux density of streams on the level $\sim 10^{10}$ W/cm².

It was found that damages of the surface layer of ferritic steels (10Cr9WV and Eurofer-97 types) under realized conditions were remarkably lower compared to those in austenitic steels. The phase compositions of ferritic steels remained steady under the pulsed action of high power density (up to 10^{10} W/cm²) and pulse durations in the range 100 ns – 1 μ s. The surface layer of tungsten after a 10-fold action of pulsed irradiation under hard conditions ($q \approx 10^{10}$ W/cm², $\tau \approx 100$ ns) was rather strongly damaged. Elongated surface cracks and significant erosion of the material were observed: the mean thickness of the layer evaporated per single pulse from the tungsten specimens was 2 μ m.

Taking into account the fact that ferritic-martensitic steels are the armour material in NFD with ICP, in plasma devices and accelerators and the basic structural materials for NFD with MCF, whereas tungsten is the armour material for the divertor plate in ITER, the results obtained are useful for preliminary estimation of the prospects for applying these materials in future thermonuclear fusion devices with magnetic and inertial plasma confinement.

It is also found that the DPF devices can be useful for preliminary treatments of materials with pulsed ion and plasma beams to improve physicochemical

and mechanical properties by means of the formation of micro- and nanoscale disperse structure and also of doping of impurity atoms on the specimen surface. The results obtained also lead to the validity of using the DPF devices in new pulsed technologies for material treatment by powerful nanosecond and microsecond pulses of radiation.

Acknowledgment. This work was partially supported by the International Atomic Energy Agency (Research Contracts nos.: 11940, 11942, 11943, 12062) Regular Budget Fund.

References

1. Borowiecki M, De Chiara P, Dubrovsky AV *et al.* (2001) Experimental study of a powerful energy flow effect on materials in PF-1000 installation. *Nukleonika* 46;S1:s117–s122
2. Burtsev VA, Gribkov VA, Filippova TI (1981) High-temperature pinch phenomena. *Itogi Nauki i Tekhniki. Fizika Plazmy* 2:80–137 (in Russian)
3. Gauster WB, Spears WR, and ITER Joint Central Team (1994) Requirements and selection criteria for plasma-facing materials and components in the ITER EDA design. *Nucl Fusion* 5;Suppl:7–18
4. Gribkov VA, Banaszak A, Bienkowska B *et al.* (2007) Plasma dynamics in PF-1000 device under the full-scale energy storage: II. Fast electrons and ions characteristics vs. neutron emission parameters, and the gun optimization properties. *J Phys D: Appl Phys* 40:3592–3607
5. Gribkov VA, Dubrovsky AV, Scholz M *et al.* (2006) PF-6 – an effective plasma focus as a source of ionizing radiation and plasma streams for application in material technology, biology and medicine. *Nukleonika* 51;1:55–62
6. Gribkov VA, Grebenshikova YeS, Demina YeV *et al.* (2008) Carbon-tungsten samples under influence of deuterium ions and dense plasma streams within plasma-focus facility. In: Proc of Int Conf Plasma 2007 on Research and Applications of Plasmas combined with the 4th German-Polish Conf on Plasma Diagnostics for Fusion and Applications and the 6th French-Polish Seminar on Thermal Plasma in Space and Laboratory, October 16–19, 2007, Greifswald, Germany. American Institute of Physics, CP 993, pp 361–364
7. Gribkov VA, Ivanov LI, Maslyaev SA *et al.* (2004) On the nature of changes in the optical characterization produced in sapphire on its irradiation with a pulsed powerful stream of hydrogen ions. *Nukleonika* 49;2:43–49
8. Gribkov VA, Pimenov VN, Ivanov LI *et al.* (2003) Interaction of high temperature deuterium plasma streams and fast ion beams with condensed materials in Dense Plasma Focus device. *J Phys D: Appl Phys* 36:1817–1825
9. Hassanein A, Konkashbaev I (1994) Erosion of plasma-facing materials during a tokamak disruption. *Nucl Fusion* 5;Suppl:193–224
10. Ivanov LI, Maslyaev SA, Pimenov VN (1999) The use of liquid metals in porous materials for diverter applications. *J Nucl Mater* 271/272:405–409
11. Ivanov LI, Pimenov VN, Maslyaev SA *et al.* (2000) Influence of dense deuterium plasma pulses on materials in Plasma Focus device. *Nukleonika* 45;3:203–207
12. Ivanov LI, Platov YuM (2002) Radiation physics of metals and applications. *Intercontact Nauka, Moscow* (in Russian)
13. Kodentsov AA, Ugaste YuE, Pimenov VN *et al.* (2003) Influence of dense deuterium plasma pulses on Fe and Fe-Mn alloy specimens in a plasma focus device. In: Proc of the Tallinn University of Social and Educational Sciences, Tallinn, B2:51–56
14. Lawrence Livermore National Laboratory (1992) Inertial confinement fusion. In: 1991 ICF Annual Report, pp 1–198
15. Martynenko YuV, Moskovkin PG, Kolbasov BN (2001) Accumulation and penetration of tritium in the firstwall of tokamak ITER in disruption regime. *Voprosy Atomnoy Nauki i Tekhniki, Series: Thermonuclear Fusion* 3:65–72 (in Russian)
16. Pimenov VN, Dyomina EV, Ivanov LI *et al.* (2002) Damage of structural materials for fusion devices under pulsed ion and high temperature plasma beams. *J Nucl Mater* 307/311;1:95–99
17. Pimenov VN, Gribkov VA, Dubrovsky AV *et al.* (2002) Influence of powerful pulses of hydrogen plasma upon materials in PF-1000 device. *Nukleonika* 47;4:155–162
18. Pimenov VN, Maslyaev SA, Demina EV *et al.* (2006) Influence of pulsed energy beams on the surface of the Al alloy tube in dense plasma focus device. *Perspektivnye Materialy* 4:43–52 (in Russian)
19. Pimenov VN, Maslyaev SA, Ivanov LI *et al.* (2003) Interaction of pulsed streams of deuterium plasma with aluminium alloy in a plasma focus device. II. Investigation of irradiated material. In: Proc of the Tallinn University of Social and Educational Sciences, Tallinn, B2:40–50
20. Pimenov VN, Maslyaev SA, Ivanov LI *et al.* (2006) Surface and bulk processes in materials induced by pulsed ion and plasma beams at Dense Plasma Focus devices. *Nukleonika* 51;1:71–78
21. Pleshivtsev NV, Bazhin AI (1998) Physics of interaction of ion beams with the materials. *Vuzovskaya kniga, Moscow* (in Russian)